ACS APPLIED MATERIALS & INTERFACES

Research Article

www.acsami.org

Modified Superparamagnetic Nanocomposite Microparticles for Highly Selective Hg^{II} or Cu^{II} Separation and Recovery from Aqueous Solutions

Karl Mandel,*[,†,‡] Frank Hutter,[†] Carsten Gellermann,[†] and Gerhard Sextl[†,‡]

[†]Fraunhofer Institute for Silicate Research (ISC), Neunerplatz 2, D97082 Würzburg, Germany

[‡]Chair of Chemical Technology of Materials Synthesis, University Würzburg, Röntgenring 11, D97070 Würzburg, Germany

Supporting Information

ABSTRACT: The synthesis of a reusable, magnetically switchable nanocomposite microparticle, which can be modified to selectively extract and recover Hg^{II} or Cu^{II} from water, is reported. Superparamagnetic iron oxide (magnetite) nanoparticles act as the magnetic component in this system, and these nanoparticles were synthesized in a continuous way, allowing their large-scale production. A new process was used to create a silica matrix, confining the magnetite nanoparticles using a cheap silica source [sodium silicate (water glass)]. This results in a well-defined, filigree micrometer-sized nanocomposite via a fast, simple, inexpensive, and upscalable process. Hence, because of the ideal size of the resulting microparticles and their comparably large magnetization, particle extraction from fluids by low-cost magnets is achieved.

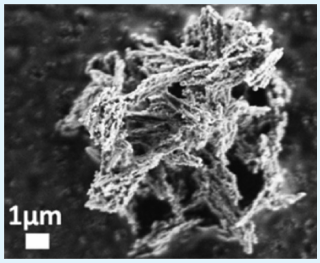

KEYWORDS: *superparamagnetism, nanocomposite, microparticle, separation, recycling*

1. INTRODUCTION

The separation of substances that are dissolved or dispersed in fluids is of great interest in many applications. Such substances may be biological in origin such as proteins[1] or cells in physiological solutions,[2] hazardous heavy-metal ions in drinking water,[3,4] or precious ions in process wastewater.[5] In the field of catalysis, recycling of valuable organic/inorganic catalysts[6,7] or enzymes in bioreactors[8−12] is desirable.[6−12] Ideally, one would like to extract the target substance and remove it from the fluid.

A smart answer to all of this is the application of magnetically separable particles, which act as carriers for the substance of interest.[1−4,6−12] Although magnetic separation has been a well-known process for a long time, nanotechnology introduced a new aspect to this technique. If magnetic particles are small (typically below 20 nm), they can become superparamagnetic.[13] These particles behave like strong magnets in the presence of an external magnetic field (like their bulk counterparts) but lose their magnetization instantly as soon as the external field is removed; i.e., they have no remanent magnetization (unlike their bulk counterparts) and therefore can be used as switchable magnets. These particles can be well dispersed in a fluid because they do not agglomerate magnetically. Therefore, if their surface is functionalized properly, they can adsorb target substances selectively and be removed by the gradient of an external magnetic field.[2,14] The exceptionally high surface-to-volume ratio of nanoparticles is clearly a further advantage.

Magnetic separation can, in principle, be simply achieved by a hand-held magnet. The magnetic force, directing the particles toward the magnet, is proportional to the magnetic field gradient, to the magnetization of the particles, and to their volume.[2,14] However, for nanodisperse particles, the randomly directed forces of Brownian motion are stronger than the magnetic forces. Thus, individual nanoparticles are usually not separable in this simple way. This is different from what is very often claimed in literature, a point recently discussed by Mandel and Hutter.[15] An increase in the particle size without a loss of superparamagnetism would greatly enhance separability because the magnetic force is proportional to the volume of the particle and the Brownian forces are negligible for larger particles. This may be achieved by assembling nanoparticles into a matrix of diamagnetic materials, forming a composite microparticle (nanocomposite).[16] All nanoparticles in the composite contribute to the magnetic attraction toward an applied field gradient, and the whole particle will be separated. However, the high specific surface area of the individual nanoparticles may be lost in that way.

Much research has been done on coating magnetic nanoparticles with a diamagnetic material, mainly silica, forming core−shell particles.[17−22] Magnetic multicore composites with a silica[23,24] or polymer[25−28] matrix, as well as hybrid combinations of polymeric and silica matrixes,[29−32] have been reported. Typically, the sizes of the composite particles reported are below 200 nm,[17−26,29−32] and their application is mainly intended for biotechnology on a laboratory scale.[20−22,24,26,27,29,31,32] Commercially available products, mostly below 1 µm, are also mainly dedicated for the biotechnology market.[2,33,34] Often the particles are dense spheres,[2,24,25,29,32,33] resulting in a small specific surface area, produced totally in very small quantities (milligrams to grams),

Received: August 2, 2012
Accepted: September 12, 2012
Published: September 12, 2012

   dx.doi.org/10.1021/am301910m | ACS Appl. Mater. Interfaces 2012, 4, 5633−5642

they come with a price of a few hundred dollars per gram. Although all composites developed so far are said to be magnetically separable, their magnetization is surprisingly low (often below 5 emu/g), which is massively lower than the expected value for magnetite (60−80 emu/g).[17,20,22,23,25,27,29−32] At sizes below 1 μm, these particles separate from solutions very slowly because of the proportionality of the magnetic forces to their small volume and low magnetization.[2,14] This is far from ideal because, in large-scale technical applications, a fast magnetic separation is necessary for a high throughput. Higher magnetization (>100 emu/g) has been reported for iron[28] or cobalt nanoparticles[35] and iron carbide composites.[36] Unfortunately, these particles show a remanent magnetization, which might lead to magnetic agglomeration, possibly hindering a proper redispersion in water after magnetic separation.

Modified magnetic particles have previously been used as scavengers for heavy-metal ions (e.g., lead, mercury, chromium, cadmium, arsenic, copper, and zinc) in water.[37−55] Apart from being toxic, heavy metals are precious resources in many industrial applications, and hence their recovery from process wastewater is highly desirable. It is often claimed that the magnetic nanoparticles used as scavengers were dispersed in water and magnetically separated by a hand-held magnet. For particles of several 100 nm in size, magnetic separation is possible but slow. Particles smaller than 100 nm show poor magnetic separability unless they are agglomerated in water; naturally enough the degree of agglomeration can vary significantly depending on the prevailing pH of the water,[56] a subject rarely investigated.[15] For Hg^{II} removal,[37−43] thiol-modified nanoparticles have proven to be good adsorbers.[39−43] However, adsorbing Hg^{II} selectively has proven to be more difficult. Using dimercaptosuccinic acid, no selectivity for Hg^{II} was observed.[39] Poly(3,4-ethylenedioxythiophene)-modified magnetic particles showed uptake of Ag^{I}, Pb^{II}, and Hg^{II}.[41] MPTS modification is suggested to be higly selective for Hg^{II}; however, it is suggested that this is not due to silane but due to the pore effects of the adsorber material.[43] Cu^{II} removal using magnetic particles has also been reported,[44−51] based on amine[44−46] or chitosan modification[47−49] or imprinting methods,[49] among others.[50,51] Selectivity is usually not considered[44−48,50,51] and is only reported for an imprinted material;[49] however, particles were not superparamagnetic in that case.

Cu^{II} extraction for large-scale mining applications is often done via liquid−liquid extraction.[57,58] Cu^{II}-selective binding molecules, such as ketoximes in a hydrophobic solvent [e.g., 2-hydroxy-5-nonylacetophenone ketoxime (LIX84, BASF) in kerosene] are mixed with water containing Cu^{II} ions. Oil−water separation allows selective extraction of Cu^{II} from the aqueous phase.[57,58] However, this method has several disadvantages including the need for large amounts of hydrophobic solvent and intense mixing, as well as cross-contamination.[57,58] Impregnations of silica gels and membranes with LIX84 have been demonstrated via the anchoring of CH groups from aminosilanes[59] or chlorosilanes[60−62] on a silica surface, which created a hydrophobic interaction between LIX84 and the CH-modified surface. Modifying magnetic particles with a selective Cu^{II} binding agent designed for solvent extraction could result in a material that is applicable for a process overcoming the disadvantages of conventional solvent extraction.

For all applications and, in particular, for water treatment utilization, magnetic composite particles have to be produced in a fast, simple, inexpensive, upscalable way and be chemically (over a wide pH range) and mechanically stable.[63,64] The magnetic component needs to exhibit superparamagnetism, and the final composite needs tohave sufficient size (micrometer scale) to be magnetically separable, along with a large surface area. With the focus on fulfilling these demands, nanocomposite microparticles were developed in this work. Their envisaged application is recycling of heavy metals from process water.

2. EXPERIMENTAL SECTION

Materials. Iron(III) chloride hexahydrate ($FeCl_3·6H_2O$, 99%+), iron(II) chloride tetrahydrate ($FeCl_2·4H_2O$, 99%+), hydrochloric acid (HCl, 36 wt %), sodium hydroxide (NaOH pellets), (3-aminopropyl)-triethoxysilane, (3-mercaptopropyl)trimethoxysilane (MPTS, 95%), and propyltrimethoxysilane (PTMS, 97%) were purchased from Sigma-Aldrich and used without further purification. An ammonium hydroxide solution (NH_4OH, 25 wt %) in water, nitric acid (HNO_3, 1 M, diluted from a 53 wt % solution), and a sodium silicate (water glass) solution ($Na_2Si_3O_7$, 36 wt %, molar ratio of SiO_2:Na_2O = 3:1) were obtained from Fischar.de Technical Chemicals and used without further purification. 2-Hydroxy-5-nonylacetophenone ketoxime (LIX84, 10% in kerosene), a selective Cu^{II} ion exchanger was obtained from BASF, U.K. For heavy-metal adsorption tests, arsenic(V) (H_3AsO_4), nitrates of cadmium(II) [$Cd^{II}(NO_3)_2·4H_2O$], zinc(II) [$Zn^{II}(NO_3)_2·6H_2O$], copper(II) [$Cu^{II}(NO_3)_2·3H_2O$], mercury(II) [$Hg^{II}(NO_3)_2·H_2O$], and lead(II) [$Pb^{II}(NO_3)_2$] as well as chlorides of chromium(III) ($CrCl_3·6H_2O$), magnesium(II) ($MgCl_2·6H_2O$), and calcium(II) ($CaCl_2$), were purchased from Sigma-Aldrich in high-purity grade.

Continuous Precipitation of Superparamagnetic Nanoparticles. A total of 8.64 g (32 mmol) of $FeCl_3·6H_2O$ and 3.18 g (16 mmol) of $FeCl_2·4H_2O$ were dissolved in 100 mL of deionized water at 20 °C. A total of 20 mL of an aqueous ammonium hydroxide solution (25 wt %) was diluted with 100 mL of water. The two solutions were mixed by pumping through 5-mm-diameter silicon tubes using a peristaltic pump (Istatec BV-GES) into a Y-shaped gas tube connection (total length 31 mm) acting as a simple continuous-flow reactor. Each arm (inner diameters of 3 mm) of the connector had a length of 18 mm; the two supporting arms met at an angle of 55°. The flow rate in each supporting channel was 100 mL/min. A black suspension formed in the outlet, from which the precipitate was separated using a hand-held permanent magnet (Supermagnet Q404020N, energy product = 42 kJ/m^3, supermagnete.de).

Stabilization of Magnetite Nanoparticles in a Sol. The precipitate (approximately 3.9 g) was washed once (dispersing it in water and magnetically separating again) and suspended in 120 mL of deionized water. The suspension was pumped through the reactor once again and thereby mixed (same conditions as before) with 120 mL of HNO_3 (0.66 M). A peptized ferrofluid was obtained at the outlet. The sol was further stabilized by carboxylic acid. The resulting sol had a pH between 1 and 2.

Formation of Composite Microparticles. *SiO_2 Precipitation.* To precipitate silica, 20 mL of a 0.5 M HNO_3 solution was mixed by stirring with 20 mL of a 25 wt % ammonium hydroxide solution. A sodium silicate solution was slowly added under stirring (molar ratio NH_4OH:HNO_3:$Na_2Si_3O_7$ = 27:1:0.4). The precipitate was filtered and washed three times. Precipitations were performed at room temperature and at 70 °C.

Matrix Formation. A total of 88 mL of 25 wt % ammonium hydroxide diluted in 80 mL of deionized water was added to the stabilized nanoparticle sol. The mixture was heated to 70 °C in air with stirring. A sodium silicate solution (molar ratio NH_4OH:HNO_3:$Na_2Si_3O_7$ as before) was added slowly through a syringe needle. The reaction mixture was stirred for 5 min at 70 °C, whereupon the product was magnetically removed and washed.

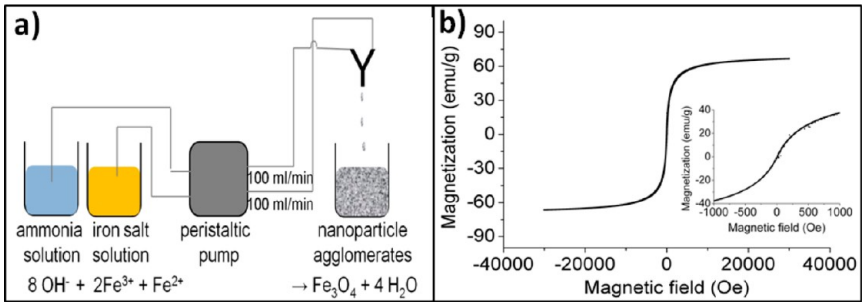

Figure 1. Continuous process for magnetite nanoparticle synthesis (a). Magnetization curve of the precipitated product (b).

Surface Modification of Composite Microparticles. (a) Thiol functionalization was achieved by the addition of 2 mL of MPTS 5 min after water glass was added to the reaction solution, forming microparticles (see before). The mixture was stirred for 1 h before magnetic separation and washing in ethanol and water.

(b) Particle modification with a Cu^{II} ion exchanger was carried out as follows: 2 g of magnetic microparticles were dispersed in 100 mL of ethanol. A total of 8 mL of aqueous ammonia (28%) was added, together with 0.5 mL of PTMS. After 1 h with stirring, the particles were magnetically separated and washed with acetone. Wet particles were immersed in LIX84 (10 wt % LIX84 in kerosine) and shaken for 1 h. Subsequently, particles were magnetically separated, washed with acetone, dried for 6 h at 130 °C, and then redispersed in water by heavy shaking.

Metal-Ion Separation and Recovery Tests. Salts of As^{V}, Cd^{II}, Cr^{III}, Zn^{II}, Pb^{II}, Cu^{II}, Hg^{II}, Mg^{II}, and Ca^{II} were dissolved in 1 L of deionized water to give a concentration of approximately 10 mg/L, respectively, 100 mg/L for each element. Exact concentrations were analyzed via inductively coupled plasma optical emission spectroscopy (ICP-OES). A defined amount of composite microparticles was added to 100 mL of a solution and stirred for a given time at room temperature. The particles were separated with a hand-held magnet, and the remaining solution was reanalyzed.

Analyses. Scanning electron microscopy (SEM) of the composite particles was carried out with a Zeiss Supra25 scanning electron microscope at 3 keV. Energy-dispersive X-ray analyses (EDX) of the particle composition were also done with the Supra 25 microscope at 15 keV at a working distance of 8 mm. Samples for transmission electron microscopy (TEM) were obtained by embedding composite particles in an epoxy resin, generating a flat surface by cross-sectional polishing (JEOL SM-09010 cross section polisher), and cutting a lamella with a focused Ga-ion beam (FEI Co. 200 3D focused ion beam quanta). TEM, high-resolution TEM (HRTEM), and scanning TEM (STEM) with EDX (STEM-EDX) were carried out using a JEOL JEM2010 microscope. The sizes of the nanoparticles were analyzed with small-angle X-ray scattering [SAXS; Saxsess from Anton Paar (Graz, Austria) with a copper anode X-ray tube]. Fourier transform infrared spectroscopy (FTIR) was carried out on KBr pellets, and diffuse-reflectance FTIR (DRIFT) spectroscopy on powder samples with a Nicolet MagnaIR760 spectrometer. X-ray diffraction (XRD) was performed on vacuum-dried powder samples (Phillips PW 1730/10). Peak assignments were carried out by relying on the International Center for Diffraction Data PDF-4 database. Dynamic light scattering (DLS) of particle dispersions was carried out with a Malvern Instruments Zeta Sizer Nano. Before and after ultrasonic treatment, Fraunhofer diffraction was done with a Malvern Mastersizer S. Solid-state ^{29}Si magic-angle-spinning nuclear magnetic resonance (MAS NMR) spectra were recorded at 22 °C on 100 mg samples with a Bruker DSX-400 NMR spectrometer using bottom-layer rotors (diameter 4 mm) of ZrO_2 (spinning rate 13 kHz; pulse length 2.0 μs; repetition time 180 s; external standard TMS, 79.5 MHz, $\delta = 0$). The specific surface area was measured by N_2 adsorption using Brunauer–Emmett–Teller (BET) analyses following DIN66131 with a Quantachrome Instruments Autosorb 3B. The chemical composition of the particles was analyzed via ICP-OES using a Varian Vista-Pro CCD Simultaneous ICP-OES after dissolution of the samples in hot hydrofluoric acid. Differential thermogravimetric analyses (DTA-TG) were carried out from room temperature to 600 °C with a Netzsch STA 449 C Jupiter DTA-TG analyzer coupled with a Netzsch Aeolos QMS403C mass spectrometer. The magnetic properties of vacuum-dried particles were studied with a vibrating sample magnetometer (VSM; VersaLabTM 3T cryogen-free VSM), cycling the applied field from −30 to +30 kOe two times with a step rate of 100 Oe/s. Detailed analyses were carried out by cycling the applied field from −5 to +5 kOe with 5 Oe/s. The temperature was set to 293 K (20 °C, room temperature).

The chemical stability of the particles was evaluated by stirring the particles for 24 h at pH 2 and 12, adjusted via HCl and NaOH, respectively, and analyzing (ICP-OES) the supernatant after magnetic separation of the particles. The particles were stirred for 2 h in concentrated HCl (36 wt %), and the change of the particle size was measured with Fraunhofer diffraction. The mechanical stability of the particles was tested by suspending the composite particles in water with a Bandelin Sonorex Super RK103 ultrasonic bath (180 W, 35 kHz) for 60 min and measuring their particle sizes with Fraunhofer diffraction. The ζ potential of the nanocomposites was measured on a Malvern Instruments Zeta Sizer Nano. The heavy-metal content in water was analyzed using a Varian Vista-Pro CCD Simultaneous ICP-OES.

3. RESULTS AND DISCUSSION

Continuous Precipitation of Superparamagnetic Magnetite Nanoparticles. Nanoparticles of magnetite (Fe_3O_4) are known as nontoxic materials with high magnetization. The synthesis of superparamagnetic magnetite nanoparticles from coprecipitation of iron(II) and iron(III) salts is a well-established one-pot process.[65] However, a continuous process is highly desirable for synthesis on a larger scale. Here, we report an easy continuous synthesis procedure without advanced equipment (such as oxygen-free inert chambers) using a Y-connection reactor (Figure 1a). Separation of the particles from the resulting suspension (approximately pH 11) and purification (redispersion in water and separation) could be done using a magnetic drum separator.

XRD of the magnetically separated, unpurified product confirms that either magnetite or γ-maghemite was obtained (Figure S1a in the Supporting Information). The primary particles are in the range of 10 ± 2 nm in size (counting 100 particles from TEM images and SAXS measurements; not shown). From reflex broadening (using the Scherrer formula),[66] a crystallite size of approximately 11 nm was calculated. The size of the crystallites fits well to the particles size; thus, it can be assumed that the particles are single crystals, which also fits well to TEM observations.

The magnetization curve for the dried particles shows superparamagnetism and a saturation magnetization of 67 emu/g (Figure 1b). BET measurements reveal a specific surface

area of 107 m^2/g, which is in good agreement with the theoretical value of 105 m^2/g for 10 nm spherical magnetite particles. However, the nanoparticles are severely agglomerated to sizes between 1 and 200 μm (Figure S1b in the Supporting Information).

Dispersion and Stabilization of Superparamagnetic Nanoparticles in a Sol. Although the agglomerated nanoparticles can be easily separated by a hand-held magnet, they cannot be used directly as magnetic carriers. The agglomerates are neither mechanically nor chemically stable and break into lumps of several hundred nanometers in size by ultrasonication or other mechanical shearing. At pH 3 or less, the particles redisperse completely.[56] To form magnetic carriers stable over a broad pH range, a homogeneous incorporation of the nanoparticles into a protective matrix is required and, therefore, the magnetite particles have to be homogenously dispersed and stabilized as a first step. The agglomerates are dispersed with diluted HNO_3 (continuous process). The resulting ferrofluidic magnetite sol (pH 1–2) is stabilized electrostatically (ζ potential of 22 mV)[56] and agglomerates either by a change of the pH of the sol or by the addition of other reactants. A more permanent stabilization (steric or electrosteric) can be achieved by either a comblike carboxylic polycarboxylate ether polymer[56] or carboxylic acids. In the stabilized sol, particles with hydrodynamic radii of 10–20 nm are present, as measured by DLS. The isoelectric point shifts from pH 6.8 for unstabilized nanoparticles to pH 8 for stabilized nanoparticles (Figure S4a in the Supporting Information). Superparamagnetism is preserved, and the saturation magnetization does not drop for the functionalized particles (VSM measurements; not shown).

Development of a Silica Matrix Formation Process for Composite Microparticles. If silica is chosen as the matrix material, tetraethoxysilane (TEOS) is normally used as the silica precursor in a sol–gel process. Reacting agglomerates of as-precipitated nanoparticles with TEOS to form a silica coating can be done in principle; however, this resulted in the formation of undefined particle agglomerates of sizes between 1 and 200 μm (Figure S2b in the Supporting Information). Herein, we incorporated stabilized and well-dispersed nanoparticles from a sol into a silica matrix (Figure 2) rather than nanoparticle agglomerates in order to obtain more well-defined composite particles.

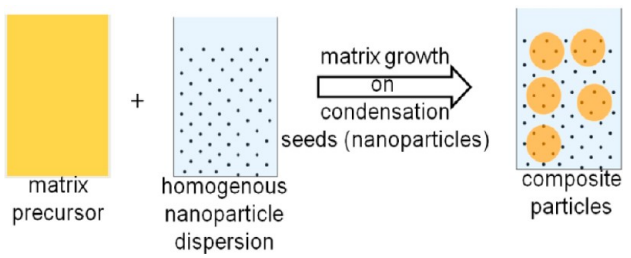

Figure 2. Processing scheme for more well-defined composite microparticles formed from a magnetite sol.

TEOS is a relatively expensive precursor for silica and led to uncontrolled gelation of the products. Using ion exchangers and careful pH adjustment, SiO_2 formation from a sodium silicate solution can be achieved for the coating of magnetic nanoparticles.[67–69] However, this process is sophisticated, slow, and hard to control. Further investigations showed that a solid silica can be obtained from simply precipitating water glass in acid.[70–72] Indeed, a precipitate is formed if water glass is added to dilute HNO_3. However, it seems that no proper silica network is obtained in that case. Solid-state ^{29}Si NMR (Figure 3a) reveals that 47% of Si atoms have a Q3 configuration (three –O–Si bonds), 29% are Q2 (two –O–Si bonds), and only 24% are Q4 (all four bonds are –O–Si). The ratio Q4/Q3 is 0.5.

The precipitate contains a remarkable amount of sodium [EDX (Figure 3b)] and dissolves immediately above pH 9. This suggests that a dense SiO_4 tetrahedral network has not been formed but that only sodium silicate is agglomerated. The specific surface area (BET) is rather small (1 m^2/g). In the presence of stabilized and dispersed magnetite nanoparticles, magnetic composite microparticles can be obtained in this way (Figure 3c,d, left). However, as expected, these composite particles are destroyed at pH values above 9 by dissolution of the matrix. The loosened magnetite nanoparticles can no longer be separated in the magnetic field gradient (Figure 3d). Furthermore, nanoparticles seem to be released from the composite during storage in water at pH 7 because after a few days the water is strongly colored and the particles are no longer magnetically well-separable. Therefore, the process is inadequate to obtain proper magnetic nanocomposite microparticles.

Stable nanocomposite microparticles were formed using a novel process.

If an aqueous ammonia solution (pH 11.5) is added to a water glass solution (pH 12), a slurry forms and quickly redissolves if diluted or stirred. Silicate anions are neutralized by NH_4^+ ions and can coagulate temporarily, but no stable Si–O–Si bonds are formed. Surprisingly, however, reasonably stable and alkali-resistant silica is precipitated if the same reaction is performed in the presence of NO_3^- ions at room temperature. At a molar ratio of $NH_4OH:HNO_3:Na_2Si_3O_7$ = 27:1:0.4, a white, honeycomb-like porous solid forms (SEM; Figure 4a). Its specific surface area is 72 m^2/g (BET). The sodium content is greatly reduced (EDX analysis; Figure 4b) in comparison to that in the acidic precipitation. The FTIR spectrum (Figure 4c) shows no absorbance for NO_3^- or NH_4^+ ions (i.e., no ammonium nitrate is formed). Only negligible amounts of nitrogen (0.43 wt %) and sodium (<3 wt %) could be detected by ICP-OES. Solid-state ^{29}Si NMR (Figure 4d) analysis results in a Q4:Q3:Q2 ratio of 33:10:1. The silica is fairly stable against dissolution even above pH 9. Even denser, and therefore more chemically stable, silica is precipitated at 80 °C. It is composed of many granular-like structures (SEM; Figure 4e). The Q4:Q3 ratio increases to 4, and no Q2 groups are present (^{29}Si NMR; Figure 4f). The specific surface area is 110 m^2/g. The temperature increase apparently promotes the formation of siloxane (Si–O–Si) bonds, strengthening the SiO_4 tetrahedral network. Some assumptions about the reaction mechanisms building up this solid silica network from a water glass solution can be found in Figure S3 in the Supporting Information.

Formation of Stable Superparamagnetic Composite Microparticles. This process of precipitating a solid silica network can be exploited to synthesize stable superparamagnetic composite microparticles in a simple, fast, and inexpensive way.

The magnetite sol prepared with the dispersing agent HNO_3 and stabilizer is mixed with aqueous ammonia. Thereby, the solution pH rises from 1 to 11.5. Agglomerates up to 1–2 μm

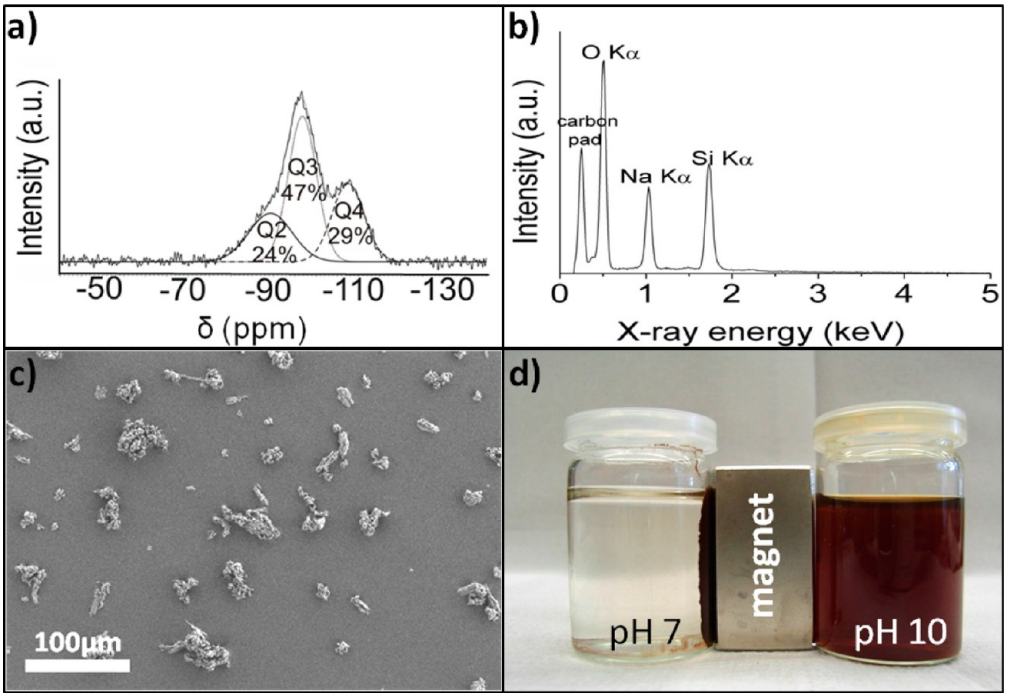

Figure 3. Silica precipitated from a water glass solution with HNO_3 (a, solid-state ^{29}Si NMR spectrum; b, EDX analysis). Magnetic composite microparticles (c, SEM micrograph) from this silica are not chemically stable and dissolve immediately by releasing nanoparticles at elevated pH values (d).

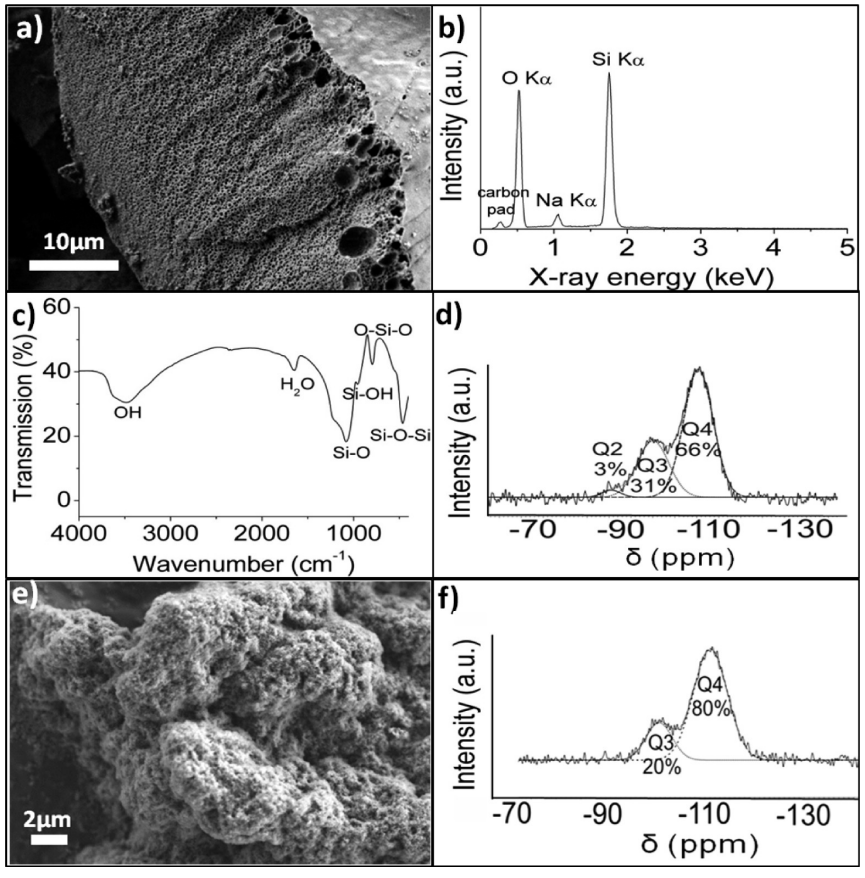

Figure 4. Foamlike, stable silica precipitated from a sodium silicate solution with aqueous ammonia in the presence of nitrate ions at room temperature (a, SEM micrograph; b, EDX analysis; c, FTIR spectrum; d, solid-state ^{29}Si NMR spectrum). Silica precipitated with the same chemicals at 80 °C (e, SEM micrograph; f, solid-state ^{29}Si NMR spectrum; EDX and FTIR equal to parts b and c).

dx.doi.org/10.1021/am301910m | ACS Appl. Mater. Interfaces 2012, 4, 5633−5642

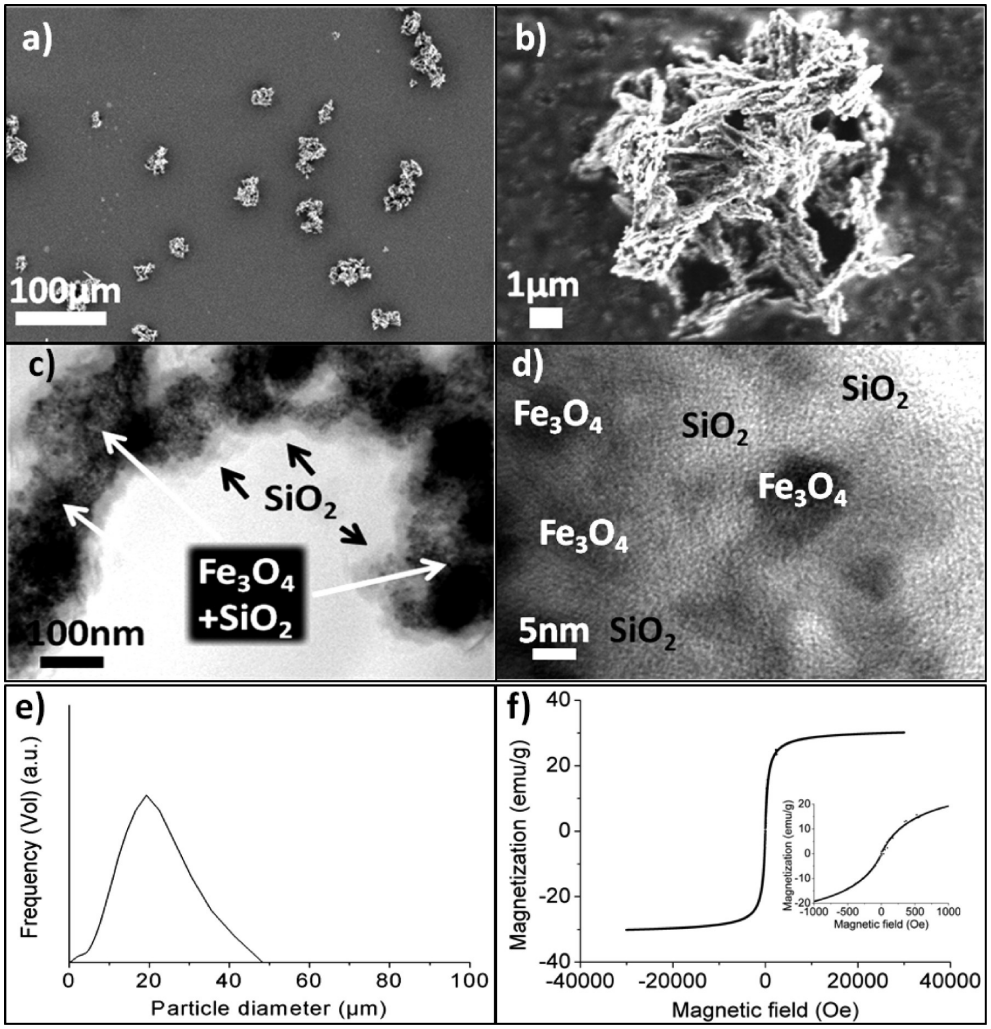

Figure 5. Superparamagnetic composite microparticles (a and b, SEM micrographs; c and d: TEM micrographs and EDX analysis; e, Fraunhofer diffraction on an aqueous suspension; f, VSM measurements).

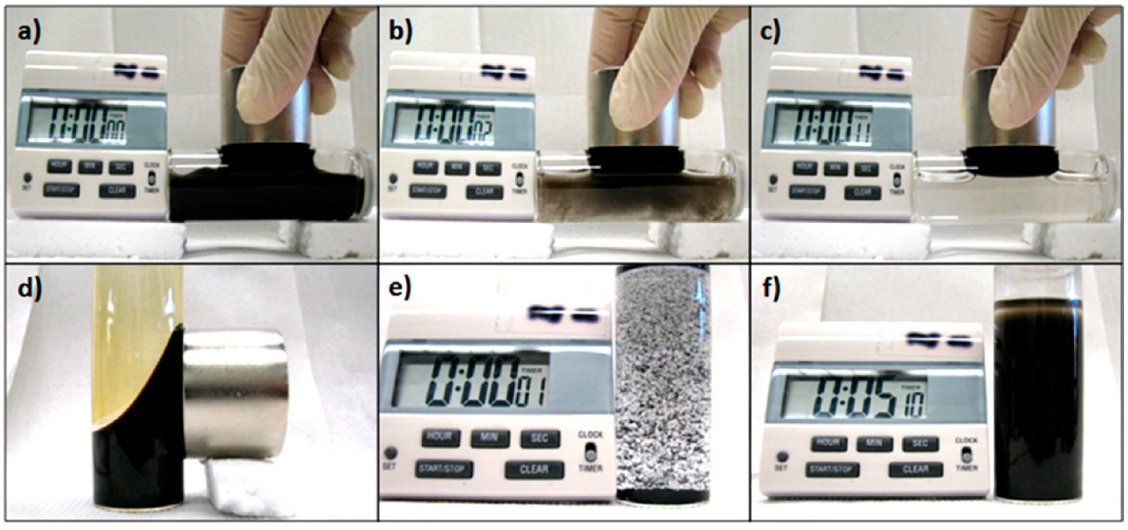

Figure 6. Magnetic separation of superparamagnetic nanocomposite microparticles (a–c). Individual nanoparticles cannot be magnetically separated from a fluid (d). Larger particles of magnetite bear remanent magnetization and immediately agglomerate if tried to redisperse in water (e). Redispersion of superparamagnetic nanocomposite microparticles does not face the problem of magnetic agglomeration (f).

(DLS) form if the dispersion is left without stirring for 1 h. However, as long as the mixture is in motion, i.e. stirred, the sol stays stable and homogeneous. After heating 70 °C, a water glass solution is added under stirring. By precipitation of SiO_2,

dx.doi.org/10.1021/am301910m | ACS Appl. Mater. Interfaces 2012, 4, 5633–5642

composite microparticles are formed. The product is separated magnetically after 5 min and washed with water. Up to 100 g of product has been synthesized in one batch. In a tube reactor and with a magnetic drum separator, the process may be continuous and upscalable.

The composite microparticles show a filigree structure (SEM micrographs: Figure 5a,b). As shown by TEM (see Figure 5c,d), a dense covering of SiO_2 surrounds and protects the magnetite nanoparticles thoroughly. STEM-EDX analysis confirms a mixture of silica and iron oxide inside the microparticle and solely SiO_2 at the surface region. That the surface of the microparticle consists only of silica can also be demonstrated by measurements of the ζ potential in dependence of the pH. The results are the same as those for pure silica [isoelectric point (IEP) at pH 2][73] and quite different from those of stabilized magnetite nanoparticles (IEP at pH 8; Figure S4a in the Supporting Information). The composition of the microparticle is also confirmed by XRD, FTIR, and EDX analyses (Figure S4b−d in the Supporting Information) and by chemical analysis (ICP-OES: 45 wt % Fe_3O_4, 50 wt % SiO_2, 5 wt % water and organic components). Upon heating of the particles to 600 °C, only water molecules are released, and no indication of chemical reactions was found (DTA-TG-MS, see Figure S4e,f in the Supporting Information). The particle-size distribution is 1−50 μm with a mean of 20 μm, which was measured by Fraunhofer diffraction for an aqueous suspension (Figure 5e). The intrinsic superparamagnetism of the magnetite nanoparticles was maintained in the microparticles (Figure 5f). Saturation magnetization of the composite particles drops to 30 emu/g from 66 emu/g of as-precipitated nanoparticles. This fits very well with the analytical composition obtained by ICP analyses. A magnetization of 30 emu/g for a micrometer-sized particle is higher than that for most composite particle systems published[17−27,29−32] and allows a fast and facile magnetic separation, an inherent precondition for industrial applications.

The superparamagnetic composite microparticles are easily separated from an aqueous suspension with a permanent magnet within 10 s (Figure 6a−c). The necessity for engineering micrometer-sized composite particles in order to obtain a magnetically separable particle system becomes evident by comparison to dispersed magnetite nanoparticles that behave like a ferrofluid and cannot be separated from the liquid (Figure 6d).[15] The advantage of the present system over larger magnetite particles is demonstrated in Figure 6e, where severe magnetic agglomeration of 500-nm-sized magnetite particles, which do not possess the nanoeffect of superparamagnetism, i.e., have a remanent magnetization, renders it impossible to properly redisperse the particles once they have been magnetized. The superparamagnetic composite particles, however, can easily be redispersed with just a gentle shake to a fairly stable suspension (Figure 6f).

The chemical stability of the composite microparticles was tested by stirring in an aqueous suspension (1.2 wt %) at pH 2 and 12 for 24 h at room temperature. After magnetic separation of the particles, the iron and silicon contents were analyzed by ICP-OES of the resulting clear, colorless solution. Almost no release of iron was detected in relation to the pH. A total of 0.16 wt % at pH 2 and 0.04 wt % at pH 12 of iron were found with respect to the total particle mass and 0.14 wt % at pH 2 and 15 wt % at pH 12 of silica, respectively. Stability against dissolution is slightly better than that for silica synthesized from TEOS (18 wt % silica dissolved at pH 12 under the same conditions). It is well-known that silica dissolution increases above pH 10.[74] Despite this partial dissolution magnetic separation of the microparticles was possible. The excellent acid resistance of the microparticles ensures that the magnetite nanoparticles are well protected at low pH. Even when particles were stirred for 2 h in concentrated HCl (36 wt %), no changes of the particle sizes were detected by Fraunhofer diffraction (not shown). The mechanical stability of the microparticles was tested by a 1 h ultrasound treatment of a 2 wt % suspension. Despite their filigree structures, the mean particle sizes increased only slightly, possibly by particles hooking together, and no breakage of the particles was observed by Fraunhofer diffraction (not shown).

A further advantage of the microparticles for any adsorption application is their large specific surface area of around 75 m^2/g (BET). Hence, because of the filigree structure of the nanocomposite, the particle's specific surface area comes close to the surface area of the 10 nm nanoparticles (100 m^2/g). The large surface area of the microparticles makes them very promising candidates for modifications, necessary for specific adsorption applications. Table 1 summarizes the characteristics of the nanocomposite microparticle system.

Table 1. Characteristics of the Nanocomposite Microparticle System

magnetic material	superparamagnetic magnetite nanoparticles 8−10 nm; continuous synthesis
matrix confining nanoparticles	amorphous SiO_2
matrix synthesis	precipitation at 70 °C from a water glass solution with ammonia in the presence of NO_3^- ions
content of magnetic nanoparticles	45 wt %
average microparticle size	20 μm
magnetization	30 emu/g
specific surface area (BET)	75 m^2/g
stability	thermal, up to 600 °C (max tested); mechanical, ultrasound stable; chemical, pH 0−12
modifications	various silanizations, impregnation

Surface Modifications of Composite Microparticles and Recovery of Hg^{II} and Cu^{II} from Aqueous Solutions. Unmodified composite microparticles adsorb metal ions from an aqueous solution unselectively to some extent, but recovery of the metals in acid is not possible. For selectivity for specific metal ions in solution and their subsequent recovery, the particle's surface was modified. To demonstrate the potential of modified particles in this respect, Hg^{II} and Cu^{II} ions were chosen as target substances, respectively.

For Hg^{II} recovery, the particle surface was modified with thiol groups using a simple reaction with a mercaptosilane. The DRIFT spectrum of the modified particles (Figure 7a) shows C−H and S−H vibrations.[42] Saturation magnetization drops from 30 to 22 emu/g. indicating a 27 wt % thiosilane modification. For selective Cu^{II} extraction, the particles were impregnated (after silanization with propylsilane) with LIX84, a molecule developed as a highly selective Cu^{II} chelating agent. The DRIFT spectrum of modified particles (Figure 7b) shows absorptions between 3200 and 3600 cm^{-1} (*p*- and *m*-hydroxyl groups), at 1400−1500 cm^{-1} (substituted benzene), and at 1600 cm^{-1} (C−N bond).[62] Magnetization drops to 16 emu/g, indicating a 47 wt % loading of the particles with LIX84 (probably including some residual kerosene). LIX84-modified

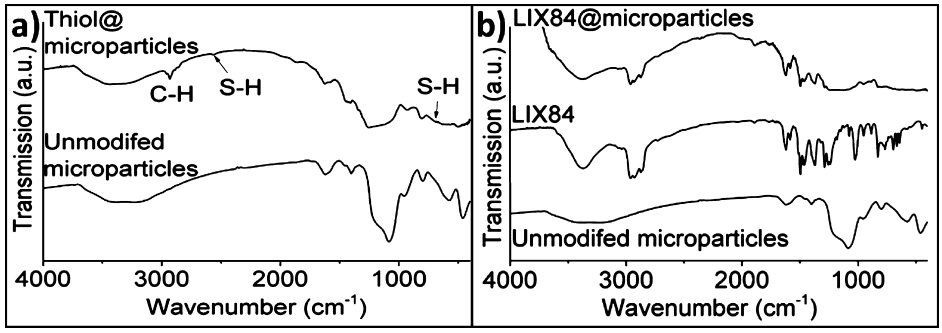

Figure 7. DRIFT spectra of thiol-modified (a) and LIX84-modified (b) magnetic particles (assignment of the peaks for unmodified microparticles can be found in Figure S4c in the Supporting Information).

composite microparticles are rather hydrophobic but disperse fairly well in water if vigorously shaken. Subsequent redispersion steps (e.g., after magnetic extraction) are easily achieved by gentle shaking.

Each particle system was dispersed at a concentration of 1 g/L in water, which contained approximately 10 mg/L of As^{V}, Cd^{II}, Cr^{III}, Hg^{II}, Cu^{II}, Zn^{II}, Pb^{II}, Ca^{II}, and Mg^{II} ions. The initial pH of the heavy-metal solution was set to 4 to avoid uncontrolled metal hydroxide precipitations. Particles were magnetically separated after a few seconds with a hand-held magnet after they were stirred for 10 min in water. Recovery (desorption) of the metal ions was carried out in 10 mL of 0.1 M HCl within 10 min before the particles were again magnetically separated, washed, and used for adsorption. The adsorption/desorption cycles were repeated three times. Concentrations of the metal ions in the adsorption/desorption solutions were determined by ICP. Data are given as percentages of the ideal (maximum possible) result (10 mg of the respective ion is adsorbed or desorbed; Figure 8).

65% Cu^{II} was adsorbed in each cycle and recovered by 66% (first cycle) to 90% (third cycle). Recovery of Hg^{II} was not possible by acid treatment alone. The addition of 2% thiourea, as suggested for modified silica,[75] seems to be the key step in the recovery of Hg^{II}. Removal of Hg^{II} of >99% was achieved for each adsorption cycle and recovered by 33%, which could not be increased by a prolonged desorption time (30 min).

As can be seen from Figure 8, adsorptions and desorptions for all other metal ions are much lower, especially in the case of Cu^{II}-adsorbing particles, which are nearly 100% selective over all other heavy metals studied. The performance of the particles does not drop within three cycles.

Cu^{II} adsorption can be increased by a longer adsorption time (30 min) to 88%. The maximum Cu^{II} capacity of the particle system is 30 mg/g (adsorption saturation reached after 1 h in a 100 mg/L aqueous heavy-metal solution). Hg^{II} adsorption was found to be >99% even after only 1 min of adsorption time. The Hg^{II} adsorption capacity of the thiol-modified particles was 74 mg/g (after 10 min of adsorption in a 100 mg/L aqueous heavy-metal solution). Only when particles are in great excess to the Hg^{II} concentration (>2 g/L per 1 mg/L Hg^{II}) are Cd^{II}, Cu^{II}, and Pb^{II} ions adsorbed as well. Hg^{II} adsorption therefore has to be considered as very fast and very much preferred.

4. CONCLUSIONS

A novel superparamagnetic nanocomposite microparticle is reported. The mechanically and chemically stable particles consist of superparamagnetic magnetite nanoparticles confined in a silica matrix. The microparticles have an ideal size for easy

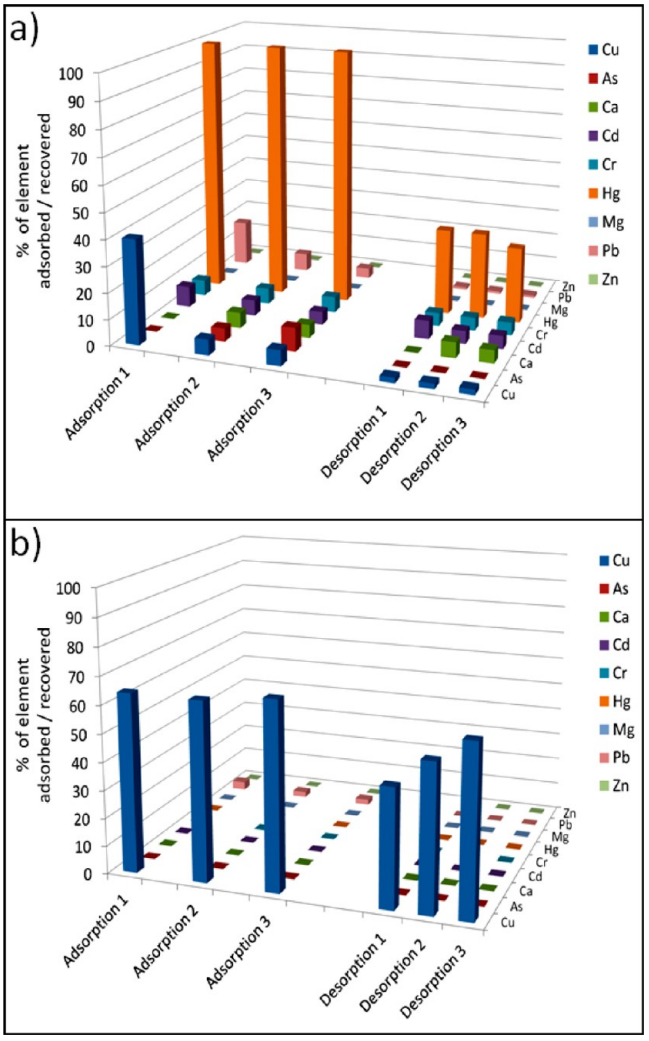

Figure 8. Results of adsorption/desorption cycles of metal ions on (a) thiol-modified and (b) LIX84-modified magnetic microparticles. 100% corresponds to the ideal (maximum possible) result.

dispersion and magnetic separation. The synthesis process is simple and fast using only inexpensive precursors and thus has great potential for upscaling. The particle's large specific surface area can be functionalized by conventional silanization, e.g., with thiol or propyl groups. Thiol-modified particles showed good adsorption selectivity for Hg^{II} over several other heavy metals in an aqueous solution. After magnetic separation, particles can be regenerated by Hg^{II} desorption in a solution of

dx.doi.org/10.1021/am301910m | ACS Appl. Mater. Interfaces 2012, 4, 5633−5642

HCl and thiourea. Cu^{II} was highly selectively extracted by and desorbed from magnetic particles impregnated with LIX84. The combination of a highly selective ion exchanger with magnetic separability provides a promising approach for processes to remove low-concentration ions in wastewater and recover and enrich them in solutions, which can be further processed to recycle the substance into a manufacturing process.

■ ASSOCIATED CONTENT

Supporting Information

Figures S1–S4. This material is available free of charge via the Internet at http://pubs.acs.org.

■ AUTHOR INFORMATION

Corresponding Author

*E-mail: karl-sebastian.mandel@isc.fraunhofer.de.

Notes

The authors declare no competing financial interest.

■ ACKNOWLEDGMENTS

We thank Alexander Reinholdt for the HRTEM images, Kathrin Bracken for TEM cuts, Werner Hopp for ICP analyses, Peter Michel for BET measurements, Andreas F. Thünemann (BAM Federal Institute for Materials Research and Testing, Berlin) for SAXS measurements, and Rüdiger Bertermann (University Wuerzburg) for solid-state ^{29}Si NMR spectra. Frank Dillon (University of Oxford, Oxford, U.K.) is highly acknowledged for very helpful discussions on this work. K.M. acknowledges the "Fonds der Chemischen Industrie (FCI)" for financial support.

■ REFERENCES

(1) Ma, Z.; Guan, Y.; Liu, H. *J. Magn. Magn. Mater.* **2006**, *301*, 469–477.
(2) Zoborowski, M.; Chalmers, J. J. *Magnetic Cell Separation*; Elsevier: Amsterdam, The Netherlands, 2008.
(3) Yavuz, C. T.; Mayo, J. T.; Yu, W. W.; Prakash, A.; Falkner, J. C.; Yean, S.; Cong, L.; Shipley, H. J.; Kan, A.; Tomson, M.; Natelson, D.; Colvin, V. L. *Science* **2006**, *314*, 964–967.
(4) Cheng, K.; Zhou, Y. M.; Sun, Z. Y.; Hu, H. B.; Zhong, H.; Kong, X. K.; Chen, Q. W. DOI: 10.1039/c2dt12312f, 2012.
(5) Chmielewski, A. G.; Urbtiski, T. S.; Migdal, W. *Hydrometallurgy* **1997**, *45*, 333–344.
(6) Schätz, A.; Hager, M.; Reiser, O. *Adv. Funct. Mater.* **2009**, *19*, 2109–2115.
(7) Shylesh, S.; Schünemann, V.; Thiel, W. R. *Angew. Chem., Int. Ed.* **2010**, *49*, 3428–3459.
(8) Gao, X.; Yu, K. M. K.; Tam, K. Y.; Tsang, S. C. *Chem. Commun.* **2003**, 2998–2999.
(9) Bahar, T.; Celebi, S. S. *Enzyme Microb. Technol.* **1998**, *23*, 301–304.
(10) Xie, W.; Ma, N. *Energy Fuels* **2009**, *23*, 1347–1353.
(11) Caruso, F.; Schüler, C. *Langmuir* **2000**, *16*, 9595–9603.
(12) Sen, T.; Bruceb, I. J.; Mercerc, T. *Chem. Commun.* **2010**, *46*, 6807–6809.
(13) Bean, C. P.; Livingston, J. D. *J. Appl. Phys. Suppl.* **1959**, *30*, 120S–129S.
(14) Ambashta, R. D.; Sillanpää, M. *J. Hazard. Mater.* **2010**, *180*, 38–49.
(15) Mandel, K.; Hutter, F. *Nano Today* **2012**, DOI: 10.1016/j.nantod.2012.05.001.
(16) Zhang, D. In *Dekker Encyclopedia of Nanoscience and Nanotechnology*, 2nd ed.; Contescu, C. I., Putyera, K., Eds.; CRC Press Inc.: Boca Raton, FL, 2008; Chapter 172.
(17) Deng, Y. H.; Wang, C. C.; Hu, J. H.; Yang, W. L.; Fu, S. K. *Colloids Surf., A* **2005**, *262*, 87–93.
(18) Kralj, S.; Makovec, D.; Čampelj, S.; Drofenik, M. *J. Magn. Magn. Mater.* **2010**, *322*, 1847–1853.
(19) Kim, K. D.; Kim, S. S.; Kim, H. T. *J. Ind. Eng. Chem.* **2005**, *11*, 584–589.
(20) Arruebo, M.; Fernández-Pacheco, R.; Velasco, B.; Marquina, C.; Arbiol, J.; Irusta, S.; Ibarra, M. R.; Santamaría, J. *Adv. Funct. Mater.* **2007**, *17*, 1473–1479.
(21) Mahtab, F.; Yu, Y.; Lam, J. W. Y.; Liu, J.; Zhang, B.; Lu, P.; Zhang, X.; Tang, B. Z. *Adv. Funct. Mater.* **2011**, *21*, 1733–1740.
(22) Salgueiriño-Maceira, V.; Correa-Duarte, M. A.; Spasova, M.; Liz-Marzán, L. M.; Farle, M. *Adv. Funct. Mater.* **2006**, *16*, 509–514.
(23) Haw, C. Y.; Chia, C. H.; Zakaria, S.; Mohamed, F.; Radiman, S.; Teh, C. H.; Khiew, P. S.; Chiu, W. S.; Huang, N. M. *Ceram. Int.* **2011**, *37*, 451–464.
(24) Piao, Y.; Burns, A.; Kim, J.; Wiesner, U.; Hyeon, T. *Adv. Funct. Mater.* **2008**, *18*, 3745–3758.
(25) Huang, Z.; Tang, F. *J. Colloid. Interface Sci.* **2004**, *275*, 142–147.
(26) Cao, Z.; Jiang, W.; Ye, X.; Gong, X. *J. Magn. Magn. Mater.* **2008**, *320*, 1499–1502.
(27) Fuertes, A. B.; Sevilla, M.; Álvarez, S.; Valdés-Solís, T.; Tartaj, P. *Adv. Funct. Mater.* **2007**, *17*, 2321–2327.
(28) Amara, D.; Grinblat, J.; Margel, S. *J. Mater. Chem.* **2010**, *20*, 1899–1906.
(29) Niu, D.; Li, Y.; Qiao, X.; Li, L.; Zhao, W.; Chen, H.; Zhao, Q.; Mac, Z.; Shi, J. *Chem. Commun.* **2008**, 4463–4465.
(30) Butterworth, M. D.; Armes, S. P.; Simpson, A. W. *J. Chem. Soc., Chem. Commun.* **1994**, 2129–2130.
(31) Niu, D.; Li, Y.; Ma, Z.; Diao, H.; Gu, J.; Chen, H.; Zhao, W.; Ruan, M.; Zhang, Y.; Shi, J. *Adv. Funct. Mater.* **2010**, *20*, 773–780.
(32) Tan, H.; Xue, J. M.; Shuter, B.; Li, X.; Wang, J. *Adv. Funct. Mater.* **2010**, *20*, 722–731.
(33) Horák, D.; Babič, M.; Macková, H.; Beneš, M. J. *Sep. Sci.* **2007**, *30*, 1751–1772.
(34) Bruce, I. J.; Taylor, J.; Todd, M.; Davies, M. J.; Borioni, E.; Sangregorio, C.; Sen, T. *J. Magn. Magn. Mater.* **2004**, *284*, 145–160.
(35) Grass, R. N.; Athanassiou, E. K.; Stark, W. J. *Angew. Chem., Int. Ed.* **2007**, *46*, 4909–4912.
(36) Herrmann, I. K.; Grass, R. N.; Mazunin, D.; Stark, W. J. *Chem. Mater.* **2009**, *21*, 3275–3281.
(37) Liu, J.; Du, X. *J. Mater. Chem.* **2011**, *21*, 6981–6987.
(38) Zhai., Y.; Duan, S.; He, Q.; Yang, X.; Han, Q. *Microchim. Acta* **2010**, *169*, 353–360.
(39) Yantasee, W.; Warner, C.; Sangvanich, T.; Addleman, R. S.; Carter, T. G.; Wiacek, R. J.; Fryxell, G. E.; Timchalk, C.; Warner, M. G. *Environ. Sci. Technol.* **2007**, *41*, 5114–5119.
(40) Song, B. Y.; Eom, Y.; Lee, T. G. *Appl. Surf. Sci.* **2011**, *257*, 4754–4759.
(41) Shin, S.; Jang, J. *Chem. Commun.* **2007**, 4230–4232.
(42) He, F.; Wang, W.; Moon, J. W.; Howe, J.; Pierce, E. M.; Liang, L. *ACS Appl. Mater. Interfaces* **2012**, *4*, 4373–4379.
(43) Jiang, Y. J.; Li, X. T.; Gao, J.; Guo, X. C.; Guan, J.; Mu, X. D. *J. Nanopart. Res.* **2011**, *13*, 939–945.
(44) Yong-Mei, H.; Man, C.; Zhong-Bo, H. *J. Hazard. Mater.* **2010**, *184*, 392–399.
(45) Tseng, J. Y.; Chang, C. Y.; Chang, C. F.; Chen, Y. H.; Chang, C. C.; Ji, D. R.; Chiu, C. J.; Chiang, P. C. *J. Hazard. Mater.* **2009**, *171*, 370–377.
(46) Lin, Y.; Chen, H.; Lin, K.; Chen, B.; Chiou, C. *J. Environ. Sci.* **2011**, *23*, 44–50.
(47) Zhou, Y. T.; Nie, H. L.; Branford-White, C.; He, Z. Y.; Zhu, l. M. *J. Colloid Interface Sci.* **2009**, *330*, 29–37.
(48) Yan, H.; Yang, L.; Yang, Z.; Yang, H.; Li, A.; Cheng, R. *J. Hazard. Mater.* **2012**, *229– 230*, 371–380.
(49) Ren, Y.; Zhang, M.; Zhao, D. *Desalination* **2008**, *228*, 135–149.
(50) Tseng, J. Y.; Chang, C. Y.; Chen, Y. H.; Chang, C. F.; Chiang, P. C. *Colloids Surf., A* **2007**, *295*, 209–216.

(51) Gong, J. L.; Wang, X. Y.; Zeng, G. M.; Chen, L.; Deng, J. H.; Zhang, X. R.; Niu, Q. Y. *Chem. Eng. J.* **2012**, *185*− *186*, 100−107.
(52) Liu, J. F.; Zhao, Z. S.; Hang, G. B. *Environ. Sci. Technol.* **2008**, *42*, 6949−6954.
(53) Huang, S. H.; Chen, D. H. *J. Hazard. Mater.* **2009**, *163*, 174−179.
(54) Hu, J.; Chen, G.; Lo, I. M. C. *Water Res.* **2005**, *39*, 4528−4536.
(55) Mayo, J. T.; Yavuz, C.; Yean, S.; Cong, L.; Shipley, H.; Yu, W.; Falkner, J.; Kan, A.; Tomson, M.; Colvin, V. L. *Sci. Technol. Adv. Mater.* **2007**, *8*, 71−75.
(56) Mandel, K.; Hutter, F.; Gellermann, C.; Sextl, G. *Colloids Surf., A* **2011**, *390*, 173−178.
(57) Kordosky, G. A. *J. South. Afr. Inst. Min. Metall.* **2002**, *11*, 445−450.
(58) Kentish, S. E.; Stevens, G. W. *Chem. Eng. J.* **2001**, *84*, 149−159.
(59) Kim, J. S.; Yi, J. *J. Chem. Technol. Biotechnol.* **1999**, *74*, 544−550.
(60) Cooper, C. A.; Lin, Y. S.; Gonzalez, M. *J. Membr. Sci.* **2004**, *229*, 11−25.
(61) Kim, J. S.; Chah, S.; Yi, J. *Korean J. Chem. Eng.* **2000**, *17*, 118−121.
(62) Cooper, C.; Lin, Y. S.; Gonzalez, M. *Ind. Eng. Chem. Res.* **2003**, *42*, 1253−1260.
(63) Franzreb, M. Magnetic separation: a selective technique for magnetic microadsorbers and catalysts. 21st Discussion Congress of Inorganic−Technical Chemistry, Germany, Frankfurt, 2012.
(64) Eichholz, C. Roadmap of magnetic separation from university research to industrial application. 21st Discussion Congress of Inorganic−Technical Chemistry, Frankfurt, Germany, 2012.
(65) Laurent, S.; Forge, D.; Port, M.; Roch, A.; Robic, C.; Elst, L. V.; Muller, R. N. *Chem. Rev.* **2008**, *108*, 2064−2110.
(66) Patterson, A. L. *Phys. Rev.* **1939**, *56*, 978−982.
(67) Philipse, A. P.; van Bruggen, M. P. B.; Pathmamanoharan, C. *Langmuir* **1994**, *10*, 92−99.
(68) Chanéac, C.; Tronc, E.; Jolivet, J. P. *J. Mater. Chem.* **1996**, *6*, 1905−1911.
(69) Yang, C.; Wang, G.; Lu, Z.; Sun, J.; Zhuang, J.; Yang, W. *J. Mater. Chem.* **2005**, *15*, 4252−4257.
(70) Ju, D. Y.; Bian, P.; Qing, G. L.; Lu, D.; He, H. *Key Eng. Mater.* **2008**, *368*, 1366−1369.
(71) Wang, J.; Zheng, S.; Shao, Y.; Liu, J.; Xu, Z.; Zhu, D. *J. Colloid Interface Sci.* **2010**, *349*, 293−299.
(72) Liu, X.; Ma, Z.; Xing, J.; Liu, H. *J. Magn. Magn. Mater.* **2004**, *270*, 1−6.
(73) Dembski, S.; Rupp, S.; Gellermann, C.; Batentschuk, M.; Osvet, A.; Winnacker, A. *J. Colloid Interface Sci.* **2011**, *358*, 32−38.
(74) Brady, P. V.; Walther, J. V. *Geochim. Cosmochim. Acta* **1989**, *53*, 2823−2830.
(75) Walcarius, A.; Delacôte, C. *Anal. Chim. Acta* **2005**, *547*, 3−13.

■ NOTE ADDED AFTER ASAP PUBLICATION

This paper was published on the Web on September 26, 2012. Revised SI was uploaded, and the corrected version was reposted on October 3, 2012.